UNIVERSITY OF CALIFORNIA SAN DIEGO

ABCA1 and ABCG1 cholesterol transporters in astrocytes regulate pain behavior in chemotherapy-induced peripheral neuropathy in mice

A Thesis submitted in partial satisfaction of the requirements
for the degree Master of Science

in

Biology

by

Jenny Lu

Committee in charge:

Professor Yury Miller, Chair
Professor Yimin Zou, Co-Chair
Professor Stacey Glasglow

2022

The Thesis of Jenny Lu is approved, and it is acceptable in quality and form for publication on microfilm and electronically.

University of California San Diego

2022

TABLE OF CONTENTS

LIST OF FIGURES

LIST OF ABBREVIATION

AIBP	ApoA-I binding protein
ApoE	Apolipoprotein E
BSA	Bovine serum albumin
CIPN	Chemotherapy-induced peripheral neuropathy
CISP	Cisplatin
CNS	Central nervous system
DRG	Dorsal root ganglion
FBS	Fetal Bovine Serum
PNS	Peripheral nervous system
PTX	Paclitaxel
TAM	Tamoxifen
TLR4	Toll-like receptor-4

ACKNOWLEDGEMENTS

First and foremost, I would like to express my sincere gratitude to my advisor, Dr. Yury Miller, for his continuous support and advice on my master's study. His patience, guidance, dynamism, motivation, and trust in my capability to study Science challenged my minds and ability to push beyond my limits to complete my thesis.

In addition, I would like to give special thanks to Dr. Juliana Navia-Pelaez who supported and guided me throughout my time in research. Her constant encouragement helped me overcome many barriers that I encountered in research. I could not have imagined a better mentor for my study.

I would like to express my deepest appreciation to everyone in the Miller lab and the Yaksh lab who offered many opportunities for me to strive as a researcher. Their rewarding professional and personal guidance taught me a great deal in scientific research.

Lastly, my sincere thanks go to the committee team, Dr. Yimin Zou and Dr. Stacey Glasglow, whose work inspired me to study glial cells. This project could not have been accomplished without their contribution and participation in the committee team.

Chapter 1, in full, is a reprint of the material as it appears in Normalization of Cholesterol Metabolism in Spinal Microglia Alleviates Neuropathic Pain. Navia-Pelaez, JMC; Choi, S.-H.; Capettini, L.S.A.; Xia, Y.; Gonen, A.; Agatisa-Boyle, C.; Delay, L.; Gonçalves dos Santos, G.; Catroli G.F.; Kim J.;, Lu, J.W.; Saylor, B.; Winkels, H.; Durant, C.P; Ghosheh, Y.; Beaton, G.; Ley, K.; Kufareva, I.; Corr, M.; Yaksh, T.L.; Miller, Y.I. *Journal of Experimental Medicine* 2021. 218(7):e220202059. DOI:10.1084/jem.20202059. The thesis author was the co-author of this paper.

VITA

2021 Bachelor of Science in Biochemistry and Cell Biology, University of California San Diego

2022 Master of Science in Biology, University of California San Diego

PUBLICATION

Navia-Pelaez, JMC; Choi, S.-H.; Capettini, L.S.A.; Xia, Y.; Gonen, A.; Agatisa-Boyle, C.; Delay, L.; Gonçalves dos Santos, G.; Catroli G.F.; Kim J.;, Lu, J.W.; Saylor, B.; Winkels, H.; Durant, C.P; Ghosheh, Y.; Beaton, G.; Ley, K.; Kufareva, I.; Corr, M.; Yaksh, T.L.; Miller, Y.I. 2021. Normalization of cholesterol metabolism in spinal microglia alleviates neuropathic pain. *Journal of Experimental Medicine* 2021. 218(7):e220202059. DOI:10.1084/jem.20202059

ABSTRACT OF THE THESIS

ABCA1 and ABCG1 cholesterol transporters in astrocytes regulate pain behavior in chemotherapy-induced peripheral neuropathy in mice

by

Jenny Lu

Master of Science in Biology

University of California San Diego, 2022

Professor Yury Miller, Chair
Professor Yimin Zou, Co-Chair

Chronic pain is a major problem restraining people from performing everyday tasks. Recent studies showed that cholesterol metabolism in microglia regulates neuropathic pain, however, little is known about the unique role astrocytes play during chronic pain. In this thesis paper, we focused on exploring two main cholesterol transporters in astrocytes, ABCA1 and ABCG1, and their roles in controlling neuropathic pain. Here, we used the chemotherapy-induced peripheral neuropathy (CIPN) model in male mice with conditional deletion of

ABCA1 and ABCG1 cholesterol transporters in astrocytes (ABC-iaKO) and male mice with constitutive deletion of apolipoprotein E (ApoE-KO) to examine their pain behavior response and analyze their glial and neuronal lipid composition using flow cytometry. We found that ABC-iaKO mice were not affected by the CIPN model and showed higher mechanical paw-withdrawal thresholds than wild-type mice. When looking into the lipid content of neurons, both ABC-iaKO and ApoE-KO mice subjected to chemotherapy treatment displayed a trend toward lower lipid droplets and lipid rafts levels compared to wild-type mice. Our findings demonstrate that ABCA1 and ABCG1 transporters in astrocytes play essential roles in regulating neuropathic pain response and possibly altering neuronal lipid content through ApoE. Through this study, we could further understand how astrocytic cholesterol regulates neuropathic pain and contribute to creating a safe treatment for chronic pain.

INTRODUCTION

Chronic pain is one of the common symptoms appearing in patients with rheumatic diseases, spinal or peripheral nerve injuries, and neuroinflammation (Ji *et al.*, 2018; Lee *et al.*, 2011). Neuroinflammation is an inflammatory response occurring in the peripheral nervous system (PNS) and central nervous system (CNS), causing many neurological diseases, including Alzheimer's disease (Habib *et al.*, 2020), Parkinson disease (Wang *et al.*, 2015), Huntington disease (Diaz-Castro *et al.*, 2019), amyotrophic lateral sclerosis (Di Giorgio *et al.*, 2007), and multiple sclerosis (Wheeler and Quintana, 2019); and neuropsychiatric diseases, including bipolar disease, depression, and autism (Ji *et al.*, 2018). During neuroinflammation, the vascular and blood brain barrier permeability increases, and the glial cells are activated, producing proinflammatory cytokines and chemokines that induce allodynic responses (Ji *et al.*, 2018; Vergne-Salle and Bertin, 2021). Mechanical or tactile allodynia is the condition when an innocuous stimulus provokes people to become extremely sensitive to light touches and feel pain at areas that are normally not painful (Lolignier *et al.*, 2014). At present, there is a lack of treatments that target chronic pain relief both safely and effectively. Although there are drug treatments that directly target neuroinflammation through inhibiting cytokines and chemokines, these treatments create side effects that increase the risk of infection after treatment and disrupt the immune system (Ji *et al.*, 2018). Therefore, it is necessary to further the study of glial cells in response to neuroinflammation to contribute to discovering a new target that can eventually develop into a new treatment.

Glial cells, specifically microglia and astrocytes, activate toll-like receptor-4 (TLR4) that are present in the membrane lipid rafts of the cells, a cholesterol-rich section of the membrane that holds increased levels of activated receptors, such as toll-like receptors and adaptor

molecules (Miller *et al.*, 2020). Upon nerve injury or chronic inflammation, TLR4 receptors in the lipid rafts of microglia enhance dimerization to initiate an inflammatory cellular response (Bruno *et al.*, 2018). Recently, our lab published a paper describing apoA-I binding protein (AIBP) as an anti-inflammatory molecule that contributes to the prevention of induced inflammation in the spinal cord (Woller *et al*., 2018; Navia-Pelaez *et al.*, 2021). Our studies found that AIBP blocks TLR4 dimerization and depletes cholesterol in the lipid rafts of microglia by transporting cholesterol out of the cell through ABCA1 and ABCG1 cholesterol transporters. This mechanism reverses allodynia in a mouse model of chemotherapy-induced peripheral neuropathy (CIPN), a common adverse effect presented in patients using antineoplastic agents that cause damage to their peripheral sensory, motor, and autonomic neurons (Zajaczkowska *et al.*, 2019). CIPN affects over 60% of patients immensely in the first three months of chemotherapy and prolongs for weeks to years after treatment (Navia-Pelaez *et al.*, 2021; Seretny *et al.*, 2014). The study has shown that AIBP has the ability to attenuate inflammation through reducing lipid rafts in spinal microglia using ABCA1 and ABCG1 cholesterol transporters, however, few studies have been done to investigate how lipid metabolism in astrocytes contributes to neuroinflammation. Therefore, we are interested in studying whether cholesterol efflux in astrocytes alters nociception during neuroinflammation.

Astrocytes, the most abundant glial cells, are similar to microglia in the context that both glial cells respond to painful conditions through activating inflammatory responses, resulting in neuropathic pain (Miller *et al.*, 2020). Astrocytes are the primary producers of apolipoprotein E (ApoE), a protein that regulates lipid metabolism by carrying and distributing cholesterol to cells in the CNS (Mahley, 2006). One main pathway by which ApoE becomes lipidated in the CNS is by binding to cholesterol transported out of the astrocytes through ABCA1 and ABCG1

cholesterol transporters (Chen *et al.*, 2012). Knowing that astrocytes are one of the main suppliers of cholesterol in the CNS, we hypothesize that when ABCA1 and ABCG1 cholesterol transporters are knocked down in astrocytes, there is decreased activity of cholesterol being export out of astrocytes. When less astrocytic cholesterol is transported out to the CNS, the amount of cholesterol carried to neurons by ApoE is reduced, thereby leading to "starvation" of neurons that require cholesterol for their structural integrity. Cholesterol depletion in neurons impairs synapse interaction between neurons, leading to desensitization of pain upon applying the CIPN model (Linetti *et al.*, 2010).

To understand the function ABCA1 and ABCG1 cholesterol transporters have in astrocytes upon induced injury, we generated a mouse model, $Abca1^{fl/fl}\,Abcg1^{fl/fl}\;Slc1a3\text{-}Cre^{ET}$, with conditional deletion of ABCA1 and ABCG1 cholesterol transporters in astrocytes (ABC-iaKO). In addition, we used available male mice with constitutive deletion of apolipoprotein E (ApoE-KO). We injected ABC-iaKO and ApoE-KO mice with cisplatin, a chemotherapy medication, to study the pain behavior response. The response was measured using von-Frey filaments to record 50% probability of hind paw withdrawal thresholds. We used flow cytometry to analyze the lipid rafts content and lipid droplets formation in astrocytes, microglia, and neurons to identify the underlying mechanism that renders the non-allodynic phenotype of ABC-iaKO and ApoE-KO mice.

CHAPTER 1

In the model of chemotherapy-induced peripheral neuropathy (CIPN), two doses of cisplatin (2.3 mg/kg/injection) were sufficient to induce severe allodynia in wild-type male mice. However, when AIBP was intrathecally injected on Day 7 in mice treated with cisplatin, their low mechanical paw-withdrawal thresholds reversed, presented in a level significantly higher than cisplatin/saline-treated mice on the same day of injection (Fig. 1.1). When looking at spinal microglia, allodynic mice exhibited significantly higher levels of TLR4 dimers and lipid rafts. On the other hand, cisplatin/AIBP-treated mice with reversed mechanical paw-withdrawal thresholds after AIBP treatment had lower levels of TLR4 dimers and lipid rafts to levels similar to naïve mice (Fig. 1.2A-B). This suggests that intrathecal AIBP was capable of reversing CIPN-associated allodynia through lowering TLR4 dimerization and lipid rafts levels in spinal microglia, which leads to the study of differential gene expression analysis of the spinal microglia that renders these phenotypes.

To examine the different genes that alter expression upon different treatments, we performed RNA sequencing to further study the transcriptome of microglia. ABCA1 and ABCG1 cholesterol transporters in microglia were downregulated in mice treated with cisplatin. In addition, ApoE was upregulated in cisplatin/saline-treated mice, suggesting the phenotypes presented in earlier experiments were related to cholesterol trafficking. We generated a mouse model, *Abca1*$^{fl/fl}$ *Abcg1*$^{fl/fl}$ *Cx3cr1-Cre*^{ERT2}, with tamoxifen-inducible deletion of ABCA1 and ABCG1 transporters in microglia (ABC-imKO), to investigate the role of microglial ABCA1 and ABCG1 cholesterol transporters in the CIPN model. Tamoxifen-treated ABC-imKO mice displayed lower mechanical paw-withdrawal thresholds after two doses of cisplatin injection. However, different from wild-type mice, these mice were irresponsive to intrathecal AIBP

injection, remaining at a low mechanical threshold throughout the experiment (Fig. 1.3A), while non-induced ABC-imKO mice had similar behaviors as wild-type mice (Fig. 1.3B). Interestingly, the levels of TLR4 dimerization and lipid rafts of naïve ABC-imKO mice were significantly higher than naïve wild-type mice and were not affected by cisplatin treatment (Fig. 1.4A-B). The results support that ABCA1 and ABCG1 cholesterol transporters in microglia are essential players in response to AIBP.

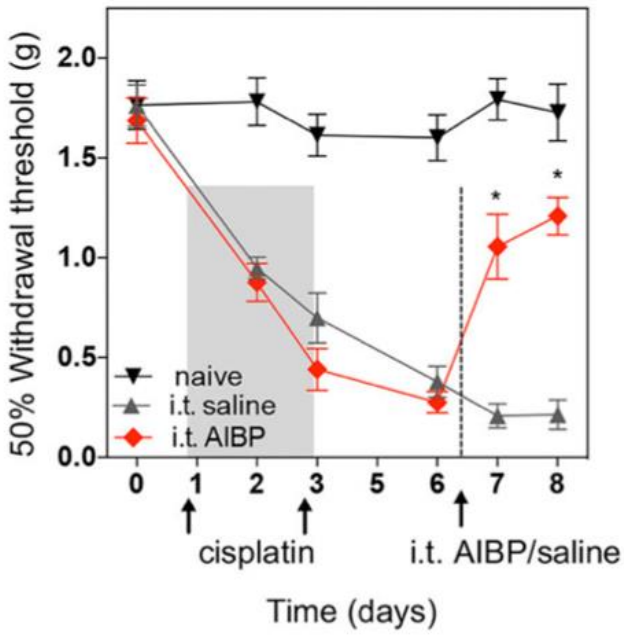

Figure 1.1: AIBP reverses allodynic response in CIPN-treated C57BL/6J mice. Male mice received two intraperitoneal injections of cisplatin (2.3 mg/kg/ injection) on Day 1 and 3 (represented by arrows), followed by a single intrathecal injection of either saline (5 µL) or AIBP (0.5 ug/5 µL) on Day 7 before measurements. Naïve mice did not received injection. (n=6 per group) Paw withdrawal thresholds were calculated based on von-Frey filaments response measurements. Two-way ANOVA was used to perform multiple comparisons of the three groups. Mean±SEM; *$P < 0.05$.

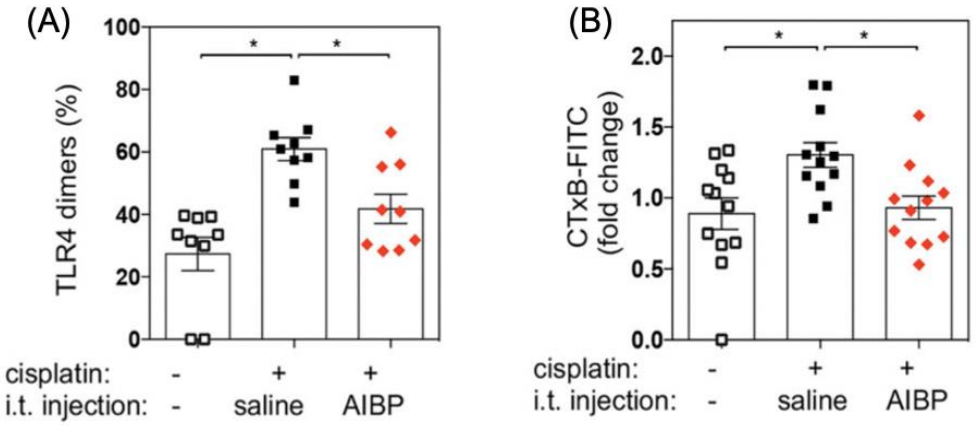

Figure 1.2: CIPN alters TLR4 dimerization and lipid rafts content in spinal microglia. Single cell suspension of spinal cord from mice was collected to perform flow analysis on Day 8 of the experiment. Flow analysis of $CD11b^{+}$/$TMEM119^{+}$ spinal microglia in **(A)** percentage of TLR4 dimers and **(B)** fold change of lipid rafts content was presented. TLR4 receptors were measured using MTS510 that recognizes TLR4/MD2 monomer and SA15-21 that recognizes TLR4 regardless of its dimerization status. Lipid rafts content was measured using cholera toxin B (CTxB-FITC) staining, which binds to ganglioside GM1. Mean±SEM; **P* < 0.05; Two-way ANOVA.

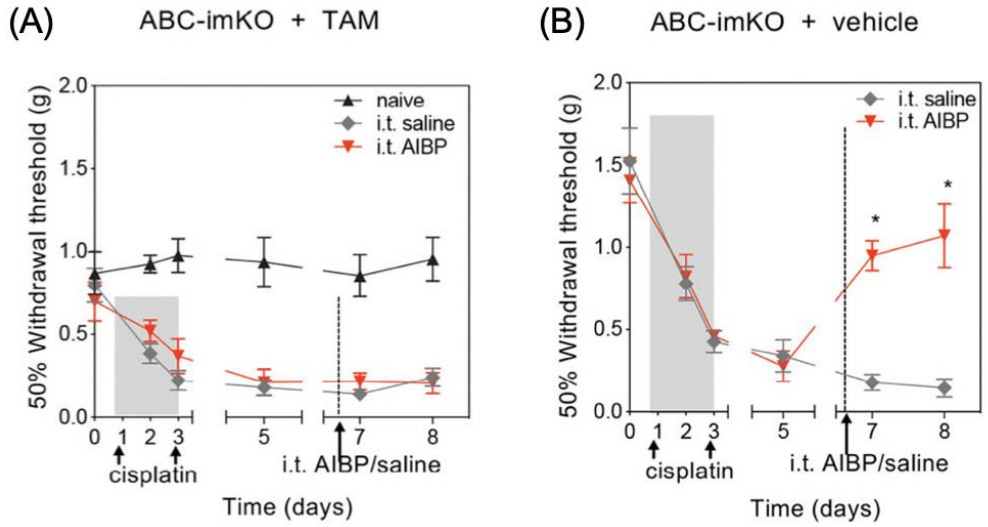

Figure 1.3: ABCA1 and ABCG1 expression in microglia regulates nociception in CIPN-treated mice. Male mice were either induced with **(A)** tamoxifen to induce deletion of ABCA1 and ABCG1 cholesterol transporters in microglia (*Abca1*$^{fl/fl}$ *Abcg1*$^{fl/fl}$ *Cx3cr1-Cre*^{ERT2} designated as ABC-imKO) or non-induced with **(B)** vehicle. Mice received two intraperitoneal injections of cisplatin (2.3 mg/kg/ injection) on Day 1 and 3 (represented by arrows), followed by a single intrathecal injection of either saline (5 µL) or AIBP (0.5 µg/5 µL) on Day 7. Naïve mice did not received injection. (n=6 per group) Paw withdrawal thresholds were calculated based on von-Frey filaments response measurements. Two-way ANOVA was used to perform multiple comparisons between groups. Mean±SEM; **P* < 0.05.

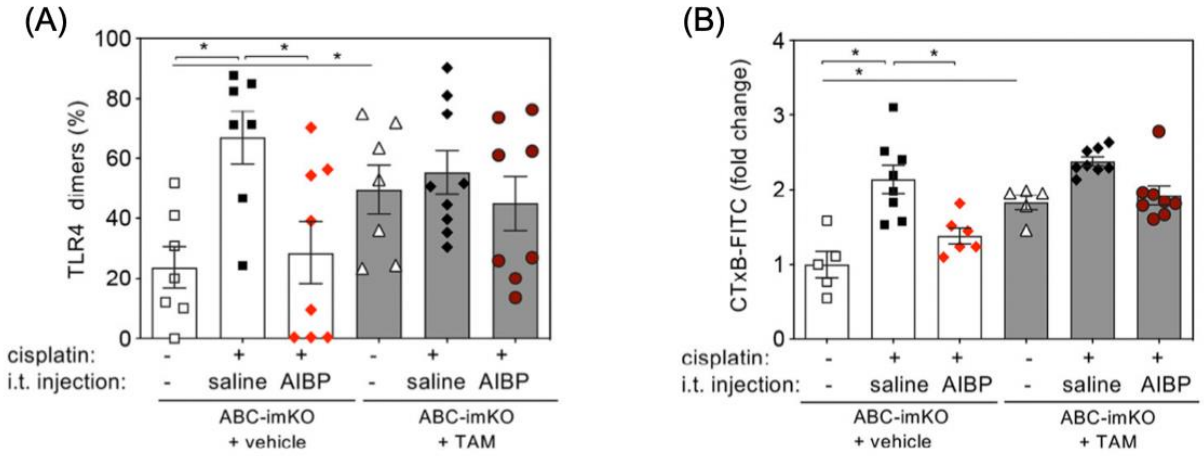

Figure 1.4: Tamoxifen-induced ABC-imKO mice are irresponsive to AIBP upon CIPN treatment. Single cell suspension of spinal cord from mice was collected to perform flow analysis on Day 8 of the experiment. Flow analysis of $CD11b^{+}/TMEM119^{+}$ spinal microglia in **(A)** percentage of TLR4 dimers and **(B)** fold change of lipid rafts content was presented. TLR4 receptors were measured using MTS510 and SA15-21 while lipid rafts content was measured using cholera toxin B (CTxB-FITC) staining. Mean±SEM; **P* < 0.05; Two-way ANOVA.

In this chapter, we observed that AIBP is capable of reversing CIPN-associated allodynia possibly through disrupting inflammarafts and TLR4 dimerization that is highly occurred on the surface of inflammatory cells. Conditional deletion of ABCA1 and ABCG1 cholesterol transporters in microglia negate the effect of AIBP, precluding AIBP from repressing inflammatory genes, leading to similar results expressed in CIPN/saline-treated mice.

Acknowledgements

Chapter 1, in full, is a reprint of the material as it appears in Normalization of Cholesterol Metabolism in Spinal Microglia Alleviates Neuropathic Pain. Navia-Pelaez, JMC; Choi, S.-H.; Capettini, L.S.A.; Xia, Y.; Gonen, A.; Agatisa-Boyle, C.; Delay, L.; Gonçalves dos Santos, G.; Catroli G.F.; Kim J.;, Lu, J.W.; Saylor, B.; Winkels, H.; Durant, C.P; Ghosheh, Y.; Beaton, G.; Ley, K.; Kufareva, I.; Corr, M.; Yaksh, T.L.; Miller, Y.I. *Journal of Experimental Medicine*

2021. 218(7):e220202059. DOI:10.1084/jem.20202059. The thesis author was the co-author of this paper.

CHAPTER 2

ABCA1 and ABCG1 cholesterol transporters in microglia have been shown to regulate nociception in cisplatin-treated mice. Both microglia and astrocytes are key targets that influence pain development; therefore, we are interested in studying whether these two cholesterol transporters in astrocytes manipulate nociception during neuroinflammation.

Reduced CIPN allodynia in ABC-iaKO mice

To obtain ABC-iaKO male mice with inducible deletion of ABCA1 and ABCG1 in astrocytes, we crossed *Abca1*$^{fl/fl}$ *Abcg1*$^{fl/fl}$ mice with *Slc1a3-Cre*^{ET} mice. Gene editing was induced by 5 daily intraperitoneal injections of 10 mg/mL of tamoxifen for five consecutive days before the start of a CIPN experiment. The CIPN model was applied in ABC-iaKO mice to induce neuropathy pain caused by chemotherapy treatment. Two cisplatin administrations (2.3 mg/kg/injection) were performed, one on Day 1 and another on Day 3. Mechanical paw-withdrawal thresholds were measured throughout the course of the experiment. Wild-type mice presented severe tactile allodynia immediately after the second injection of cisplatin that lasted throughout the experiment (Fig. 2.1A). On the other hand, ABC-iaKO mice exhibited significantly higher mechanical paw-withdrawal thresholds and area under the curve compared to wild-type mice and remained at a relatively stable withdrawal threshold before and after cisplatin treatment (Fig. 2.1B). ABCA1 and ABCG1 knockdown was confirmed in flow cytometry analysis (Fig. 2.2). These results suggest that by deleting ABCA1 and ABCG1 cholesterol transporters, ABC-iaKO mice were protected from allodynia induced by cisplatin treatment. This leads to a question of the effect deleting ABCA1 and ABCG1 cholesterol

transporters has on the cholesterol composition of astrocytes, neurons, and microglia in ABC-iaKO mice.

Compared to wild-type mice, deletion of ABCA1 and ABCG1 transporters in spinal astrocytes did not affect the level of TLR4 dimerization. However, ABC-iaKO mice exhibited significantly reduced lipid droplets level in microglia (Fig. 2.3G) and lipid rafts level in astrocytes (Fig. 2.3B). Interestingly, ABC-iaKO mice exhibited a trend toward lowered lipid droplets and lipid rafts content in neurons (Fig. 2.3D,E), suggesting that removing ABCA1 and ABCG1 cholesterol in astrocytes may contribute to regulating lipid transport and composition of neurons.

To test whether ABC-iaKO mice were only protected from cisplatin, paclitaxel (PTX), another type of chemotherapy drug (Taxol) that induces neuropathic pain, was intraperitoneally injected (8 mg/kg/injection) into mice twice on Day 1 and 3. Mechanical paw-withdrawal thresholds were measured throughout the experiment until Day 16. After two doses of paclitaxel, compared to wild-type (+ PTX) mice, ABC-iaKO (+ PTX) mice displayed significantly higher mechanical paw-withdrawal thresholds on Day 3 (Fig. 2.4). Throughout the experiment, ABC-iaKO (+ PTX) mice remained at relatively stable mechanical paw-withdrawal thresholds, with the same behavior as mice with no paclitaxel injection and mice from the same genotype with cisplatin injections (Fig. 2.1). However, there was no significant findings when observing the level of TLR4 dimerization, lipid droplets, and lipid rafts in glial cells and neurons of the spinal cord nor in immune and non-immune cells in dorsal root ganglion (Fig. 2.6-2.7). A possible explanation is that the analytical approaches we used to measure the interaction between astrocytes and neurons were not optimal. We applied similar methods to study astrocytes as we utilized with microglia and did not explore different mechanisms that may play a role in response

to the alteration of cholesterol metabolism in astrocytes. In future studies, we will design an astrocyte-specific approach to study the mechanisms underlying the allodynia-protected phenotype of ABC-iaKO mice.

One major limitation in this PTX experiment is the lack of data to validate the knockdown of both ABCA1 and ABCG1 transporters in astrocytes (Fig. 2.5). Typically, we expect to see the expression of ABCA1 and ABCG1 proteins reduced using the inducible *cre/lox* system; however, this scenario was not supported by the flow cytometry analysis, showing a trend toward reduction of ABCG1, but not ABCA1 expression. In the future, we can attempt using quantitative polymerase chain reaction (qPCR) to measure the expression of ABCA1 and ABCG1 transporters in isolated astrocytes.

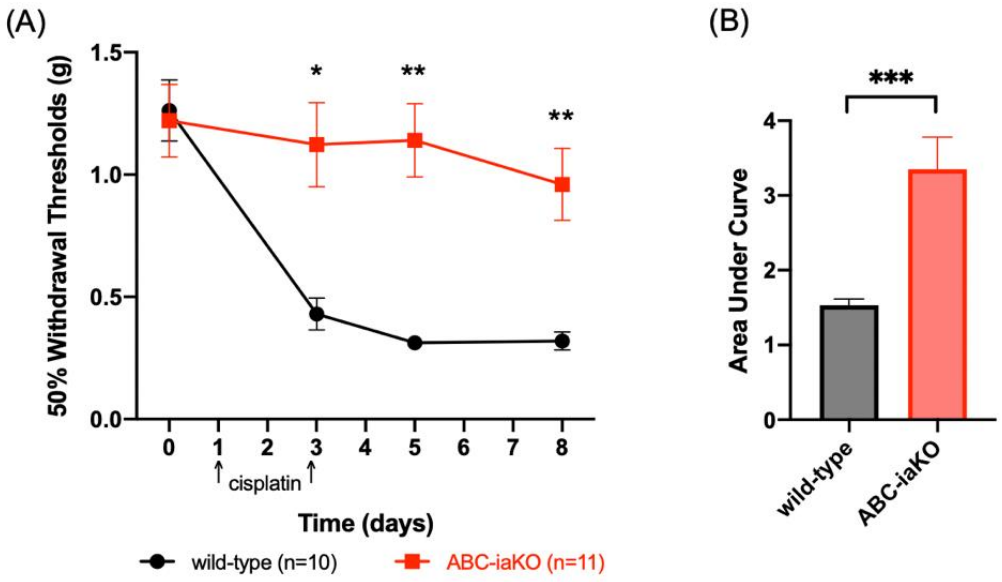

Figure 2.1: ABC-iaKO mice are protected from cisplatin-induced allodynia. Male mice with tamoxifen-inducible deletion of ABCA1 and ABCG1 cholesterol transporters in astrocytes (*Abca1*$^{fl/fl}$ *Abcg1*$^{fl/fl}$ *Slc1a3-Cre*^{ET} designated as ABC-iaKO) are prevented from developing allodynia in a model of chemotherapy-induced peripheral neuropathic pain (CIPN) using cisplatin. **(A)** Wild-type mice (n=10) and ABC-iaKO mice (n=11) were given two intraperitoneal injections of cisplatin (2.3 mg/kg/injection) on Day 1 and 3 (represented by arrows). Mechanical paw withdrawal thresholds were calculated based on von-Frey filaments response measurements. (B) Area under the curve from Day 0 to Day 8 was calculated. Mean±SEM; **P* < 0.05, ***P* < 0.005, ****P* < 0.001; two-way ANOVA in (A) and unpaired t-test in (B).

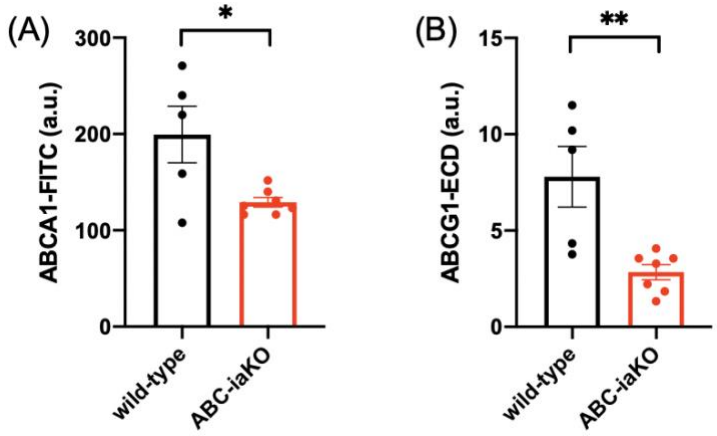

Figure 2.2: ABCA1 and ABCG1 cholesterol transporters are successfully knocked down in spinal astrocytes of ABC-iaKO mice. Single cell suspensions of the brain from wild-type (n=5) and ABC-iaKO (n=7) mice were collected to perform flow analysis on Day 8 of the experiment. **(A)** ABCA1 transporters were measured using FITC-conjugated antibody and **(B)** ABCG1 transporters were measured using ECD-conjugated antibody. Integrated intensity values were calculated by multiplying frequency of positive cells with the geometric mean of fluorescence. Mean±SEM; unpaired t-test.

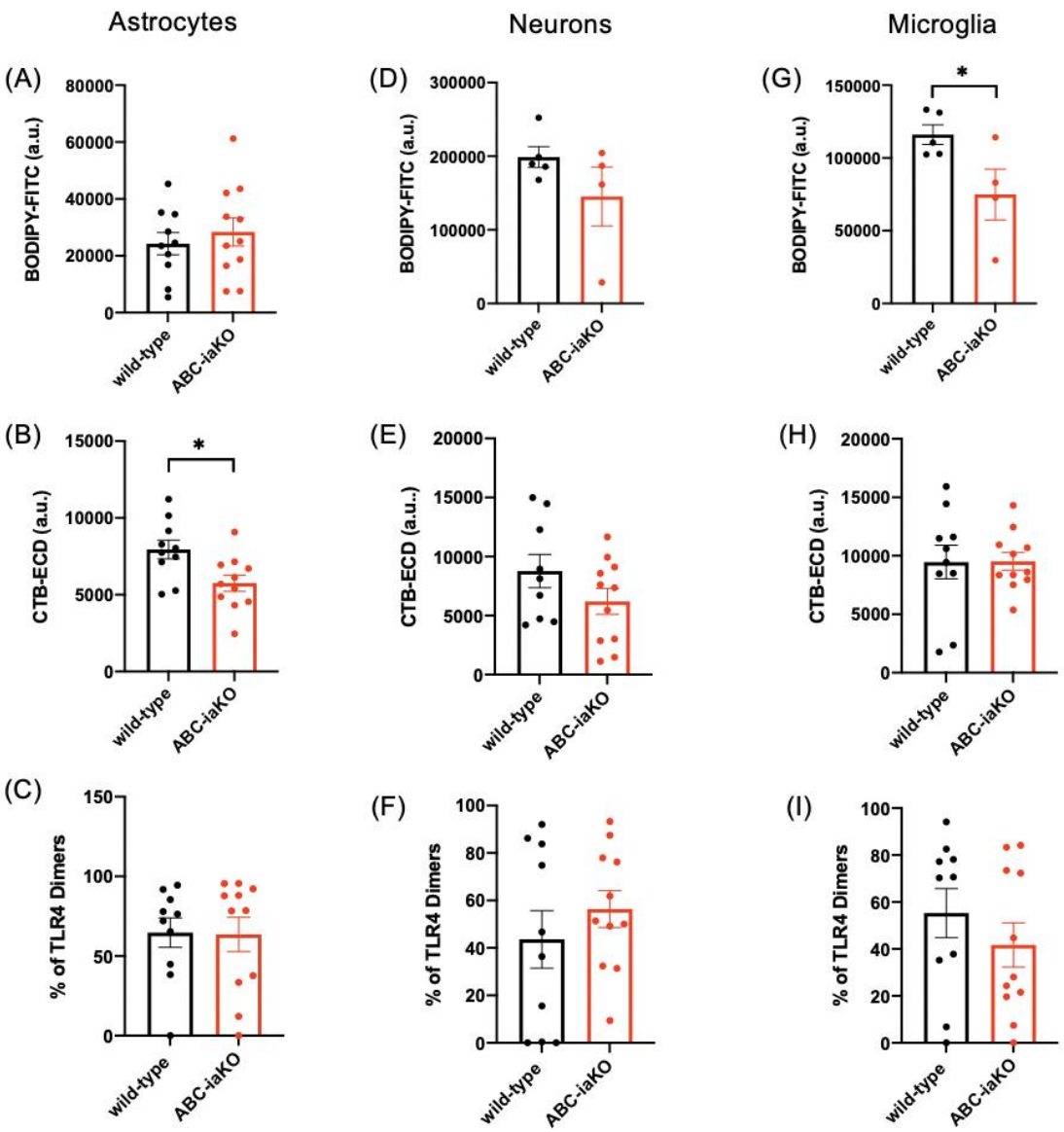

Figure 2.3: ABC-iaKO mice display a trend toward reduced lipid droplets and lipid rafts levels in neurons. Single cell suspensions of spinal cord from wild-type mice and ABC-iaKO mice were collected to perform flow analysis on Day 8 of the experiment. (**A,D,G**) Lipid droplets were measured using BODIPY-FITC staining. (**B,E,H**) Lipid rafts content was measured using cholera toxin B (CTxB-ECD) staining, which binds to ganglioside GM1. Integrated intensity values were calculated by multiplying frequency of positive cells with the geometric mean of fluorescence. (**C,F,I**) TLR4 receptors were measured using MTS510 that recognizes TLR4/MD2 monomer and SA15-21 that recognizes TLR4 regardless of its dimerization status. Data were collected from two independent experiments, except (**d**) and (**g**) from one experiment. Mean±SEM; *$P < 0.05$; unpaired t-test.

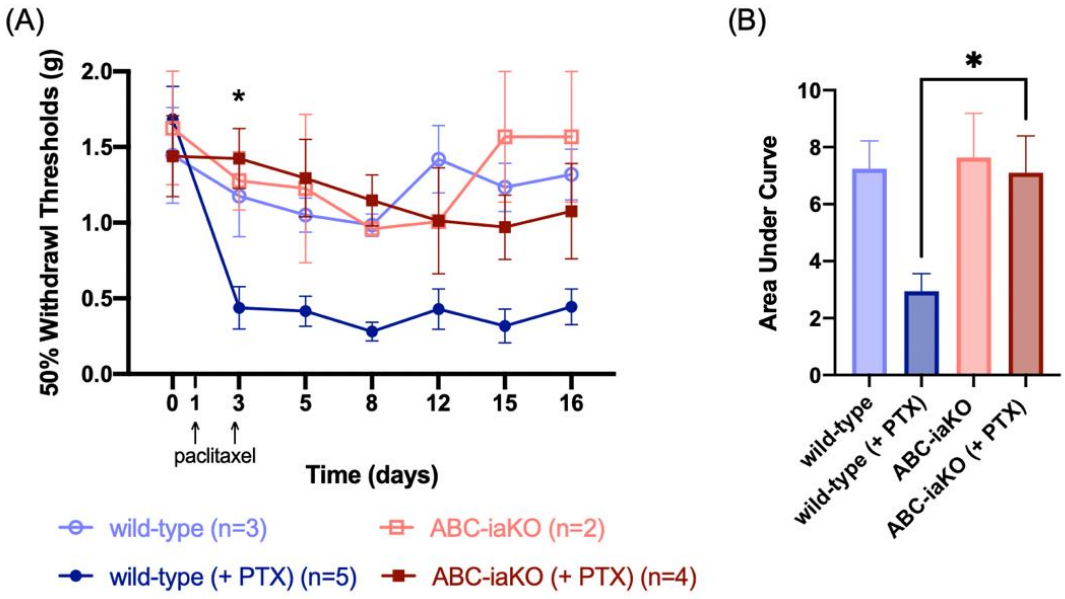

Figure 2.4: ABC-iaKO mice are protected from developing allodynia in the CIPN model using paclitaxel (PTX). Male wild-type mice (n=5; n=3) and ABC-iaKO mice (n=4; n=2) were either given two intraperitoneal injections of paclitaxel (8 mg/kg/injection; designated as + PTX) or no injection on Day 1 and 3 (represented by arrows). **(A)** Mechanical paw withdrawal thresholds were calculated based on von-Frey filaments response measurements. **(B)** Area under the curve from Day 0 to Day 16 was calculated. Mean±SEM; *$P < 0.05$; two-way ANOVA in (A) one-way ANOVA in (B).

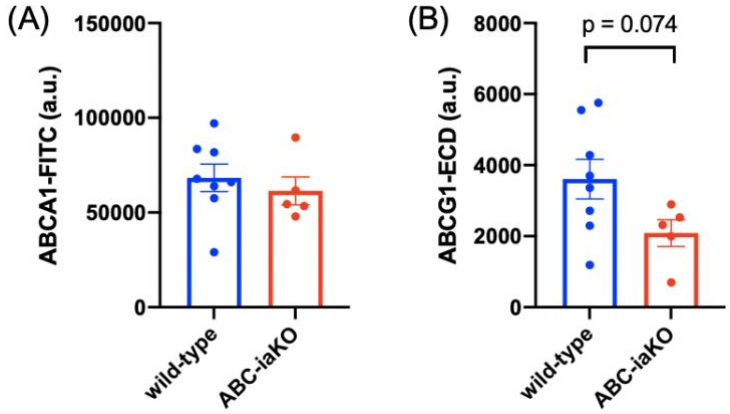

Figure 2.5: ABCA1 and ABCG1 cholesterol transporters knockdown confirmation in astrocytes. Single cell suspensions of the brain from wild-type and ABC-iaKO mice were collected to perform flow analysis on Day 16 of the experiment. **(A)** ABCA1 transporters were measured using FITC-conjugated antibody and **(B)** ABCG1 transporters were measured using ECD-conjugated antibody. Integrated intensity values were calculated by multiplying frequency of positive cells with the geometric mean of fluorescence. Mean±SEM; unpaired t-test.

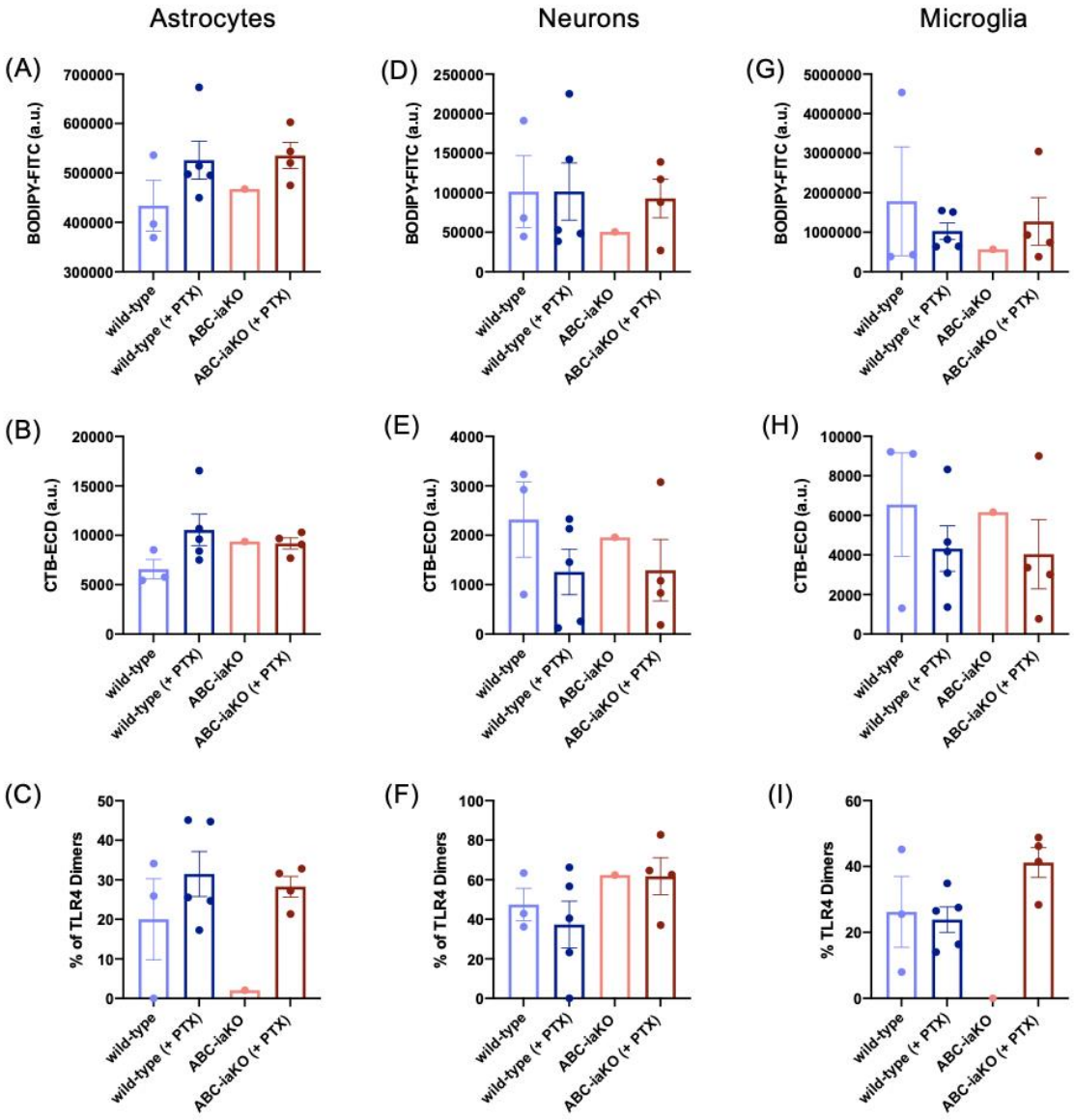

Figure 2.6: Lipid droplets, lipid rafts, and TLR4 dimerization in the spinal cord of ABC-iaKO mice. Single cell suspensions of spinal cord from wild-type mice and ABC-iaKO mice were collected to perform flow analysis on Day 16 of the experiment. **(A,D,G)** Lipid droplets were measured using BODIPY-FITC staining. **(B, E, H)** Lipid rafts content was measured using CTxB-ECD staining. Integrated intensity values were calculated by multiplying frequency of positive cells with the geometric mean of fluorescence. (**C,F,I**) TLR4 receptors were measured using MTS510 and SA15-21. One sample from ABC-iaKO mice was lost during processing. Mean±SEM; one-way ANOVA.

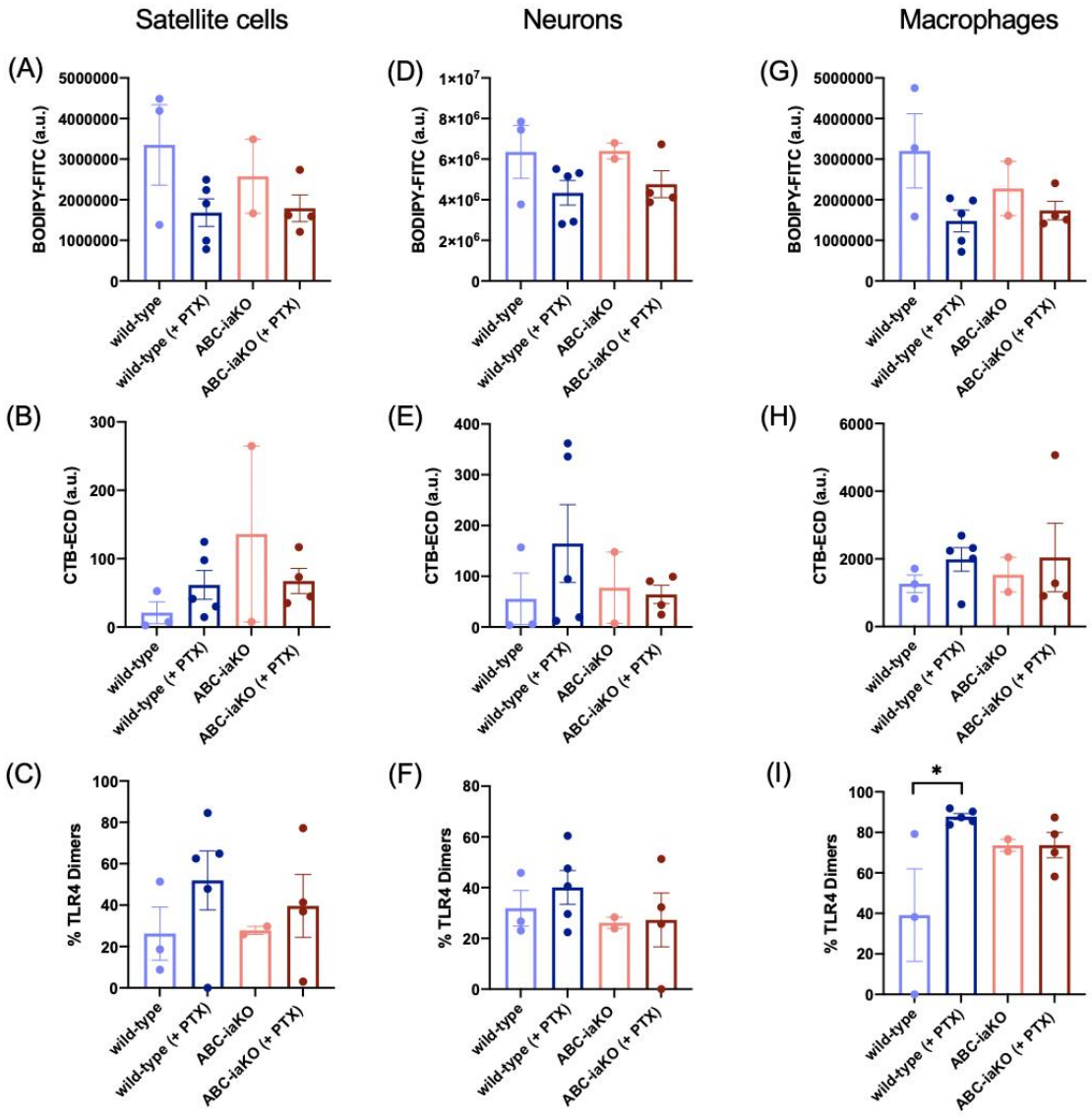

Figure 2.7: Lipid droplets, lipid rafts, and TLR4 dimerization in DRG of ABC-iaKO mice. Single cell suspensions of DRG from wild-type mice and ABC-iaKO mice were collected to perform flow analysis on Day 16 of the experiment. (**A,D,G**) Lipid droplets were measured using BODIPY-FITC staining. (**B,E,H**) Lipid rafts content was measured using CTxB-ECD staining. Integrated intensity values were calculated by multiplying frequency of positive cells with the geometric mean of fluorescence. (**C,F,I**) TLR4 receptors were measured using MTS510 and SA15-21. Mean±SEM; *$P < 0.05$; one-way ANOVA.

The deficiency in ABCA1 and ABCG1 cholesterol transporters in astrocytes protect ABC-iaKO mice from allodynia induced by cisplatin and paclitaxel treatments. We hypothesize that by deleting ABCA1 and ABCG1 cholesterol transporters in astrocytes, less cholesterol is

transported out of astrocytes to lipidate ApoE, the main cholesterol carrier in the CNS. When less cholesterol is transported to neurons, disrupting the structure of neurons, it desensitizes neurons from nociceptive signaling (Linetti *et al.*, 2010; Fig. 2.8). To test this hypothesis, the CIPN model was applied to study the allodynic response of ApoE-KO mice.

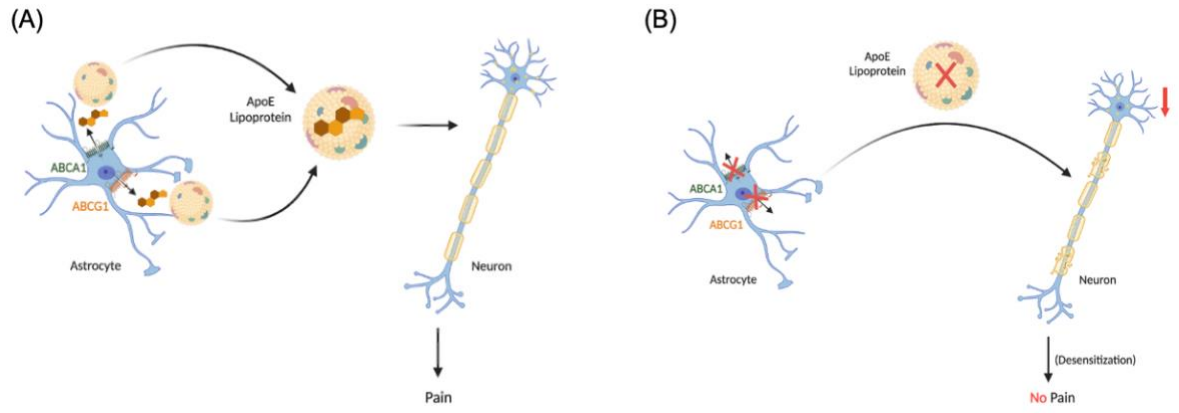

Figure 2.8: Cholesterol is transported out of astrocytes through ABCA1 and ABCG1 cholesterol transporters to ApoE lipoproteins and shuttles to neurons. Depletion of ABCA1 and ABCG1 could possibly disrupts the lipid composition of neurons, limiting the neurons' sensitivity to respond to nociception.

Reduced CIPN allodynia in ApoE-KO mice

Next, we tested the hypothesis that ApoE deficiency would have a similar CIPN non-allodynic phenotype as ABC-iaKO mice. Two doses of cisplatin were administered on Day 1 and 3. Mechanical paw-withdrawal thresholds were measured until Day 16. After the second injection of cisplatin, both wild-type (+ cisp) and ApoE-KO (+ cisp) mice experienced a drop in mechanical paw-withdrawal thresholds (Fig. 2.9A-B). However, ApoE-KO (+ cisp) mice exhibited slightly higher mechanical paw-withdrawal thresholds and significantly higher area under the curve in comparison to wild-type (+ cisp) mice throughout the course of the experiment.

In comparison to wild-type mice, lipid rafts level was decreased in astrocytes of ApoE-KO (+ cisp) mice (Fig. 2.10B). Neurons in ApoE-KO (+ cisp) mice expressed lower lipid droplet levels compared to wild-type (+ cisp) mice (Fig. 2.10D). ApoE-KO mice, regardless of cisplatin treatment, expressed a trend toward reduced lipid rafts content in neurons and lowered levels of lipid droplets and lipid rafts in microglia compared to wild-type mice (Fig. 2.10E,G-H). The levels of TLR4 dimerization in astrocytes, neurons, and microglia were similar across all four groups, suggesting TLR4 dimerization does not play a role in regulating nociception in ApoE-KO mice (Fig. 2.10C,F,I).

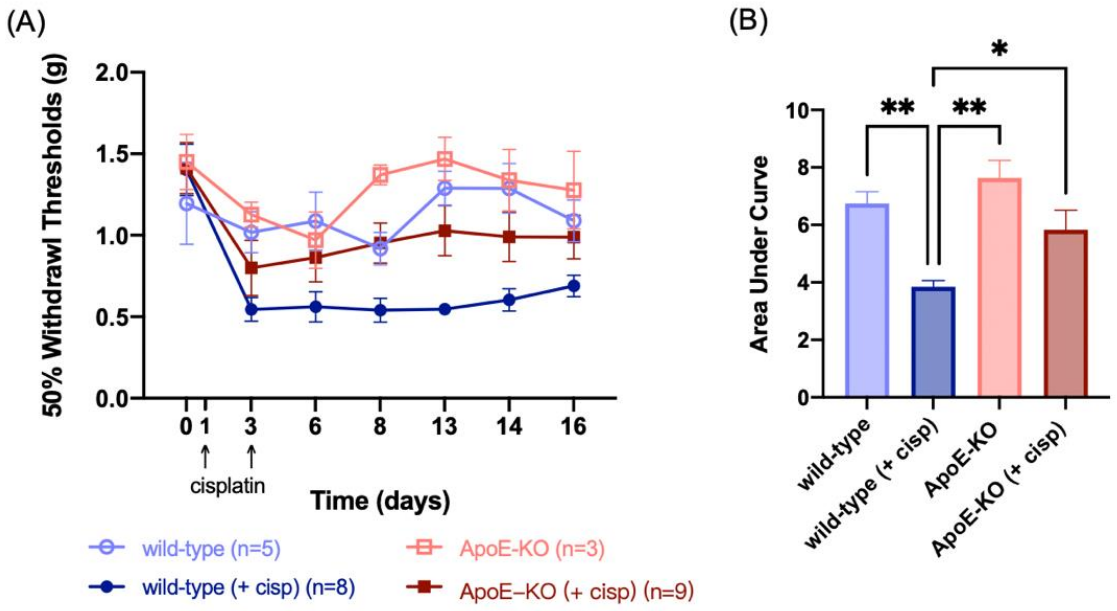

Figure 2.9: Different CIPN response in ApoE-KO and wild-type mice. **(A)** Wild-type mice (n=5; n=8) and C57BL/6J male mice with constitutive deletion of ApoE (designated as ApoE-KO; n=3; n=9) were either given no cisplatin injections or two intraperitoneal injections of cisplatin (+ cisp) (2.3 mg/kg/injection) on Day 1 and 3 before measurements (represented by arrows). Mechanical paw withdrawal thresholds were measured through Day 16. **(B)** Area under the curve from Day 0 to Day 16 was calculated. Mean±SEM; *$P < 0.05$, ** $P < 0.01$; two-way ANOVA in (A) one-way ANOVA in (B).

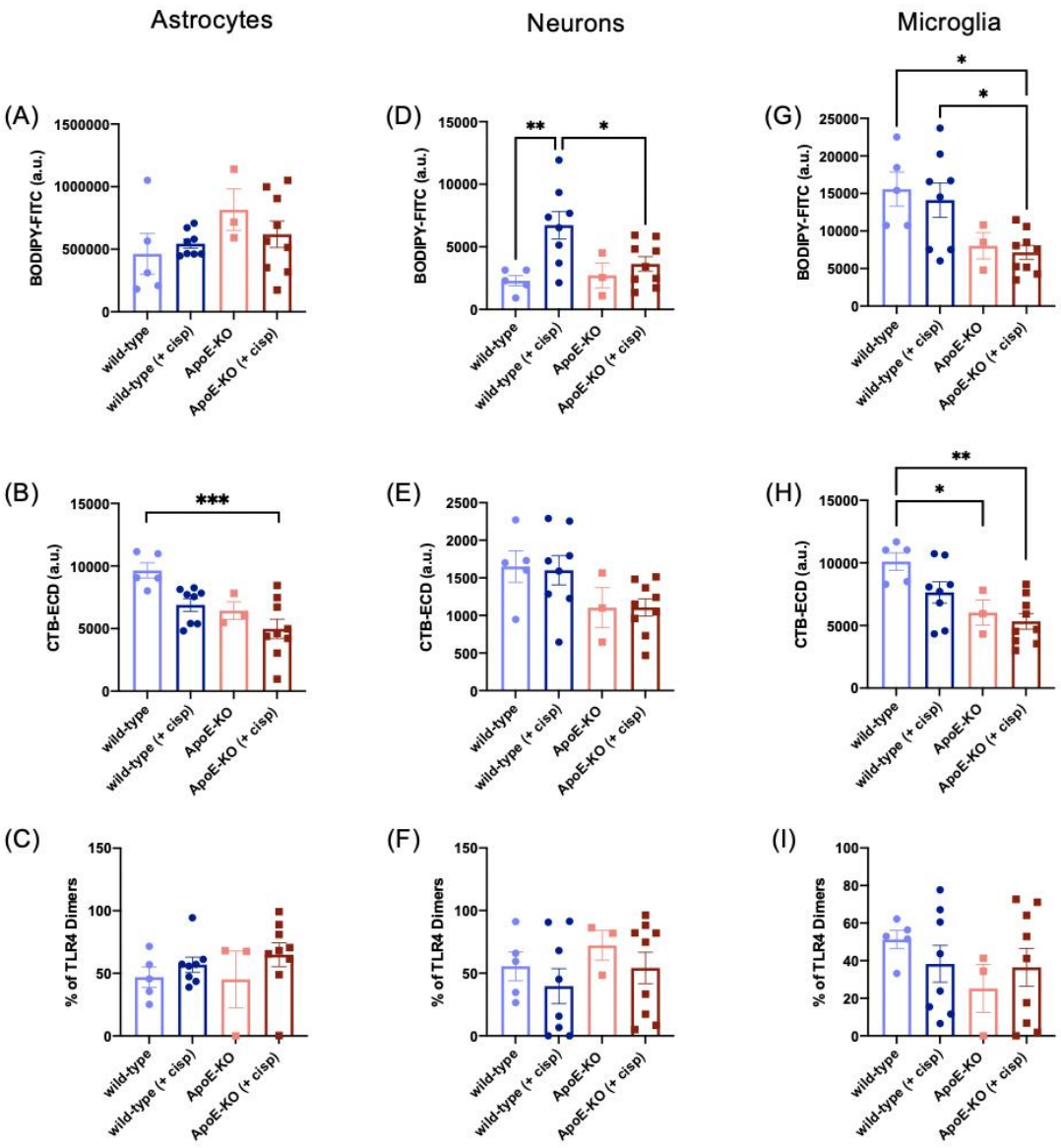

Figure 2.10: ApoE-KO mice display reduced lipid droplets and lipid rafts levels in microglia and neurons. Single cell suspensions of spinal cord from wild-type mice and ApoE-KO mice were collected to perform flow analysis on Day 16 of the experiment. (**A,D,G**) Lipid droplets were measured using BODIPY-FITC staining. (**B,E,H**) Lipid rafts content was measured using CTxB-ECD staining. Integrated intensity values were calculated by multiplying frequency of positive cells with the geometric mean of fluorescence. (**C,F,I**) TLR4 receptors were measured using MTS510 and SA15-2. Mean±SEM; **P* < 0.05, ***P* < 0.005, ****P* < 0.001; one-way ANOVA.

ApoE is a critical cholesterol transporter in the CNS. By constitutively removing ApoE, ApoE-KO mice exhibited reduced levels of lipid droplets and lipid rafts in both microglial and neuronal cells, suggesting ApoE regulates cholesterol transportation to both cell types in the

CNS. The alterations of lipid composition in microglia and neurons could possibly be the explanation to why wild-type mice were more heavily affected by cisplatin compared to ApoE-KO mice.

ApoE lipidation

When ABCA1 and ABCG1 cholesterol transporters are deleted in astrocytes, less cholesterol is transported out of astrocytes. Therefore, we expect to see less free cholesterol in the culture media of astrocytes isolated from ABC-iaKO compared to wild-type. To optimize the measurement of free cholesterol in the extracellular fluid, we incubated immortalized astrocytes with bovine serum albumin (BSA), fetal bovine serum (FBS), and human recombinant ApoE3. After the incubation, the ApoE-containing media conditioned had a significantly higher level of free cholesterol compared to control media (Fig. 2.11), illustrating the efficacy of the ApoE lipidation assay.

To study the interaction between ABCA1 and ABCG1 cholesterol transporters in astrocytes and ApoE, primary astrocytes were isolated from wild-type, ABC-iaKO, and ApoE mice to measure the level of free cholesterol in the extracellular fluid. When measuring the purity of the culture, non-immune cells and astrocytes were highly expressed, however, not exclusively (Fig. 2.12A-B). Primary astrocytes were incubated with 4'hydroxytamoxifen (4'OHT) to induce Cre^{ER}-mediated gene knockdown *in-vitro*. Using flow analysis, we found that 4'OHT did not influence the viability of cultured astrocytes (Fig. 2.13). However, astrocytes isolated from ABC-iaKO expressed higher levels of ABCA1 and lower levels of ABCG1 cholesterol transporters upon 4'OHT treatment, demonstrating the knockdown of the two transporters was not effective (Fig. 2.14A-B). In future studies, we will extend the incubation time or increase the concentration of 4'OHT used to improve the knockdown efficiency. After

successfully removing ABCA1 and ABCG1 transporters in astrocytes, we will repeat the ApoE lipidation assay with primary astrocytes isolated from wild-type and ABC-iaKO mice. We expect to see lower concentration of free cholesterol in media conditioned with ABC-iaKO astrocytes in comparison to wild-type astrocytes due to less cholesterol is being transported out of the astrocytes through the two transporters to lipidate ApoE.

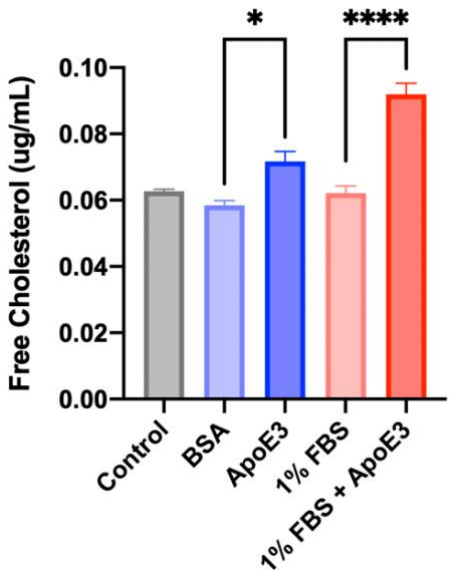

Figure 2.11: Optimization of ApoE lipidation assay. Immortalized astrocytes were incubated with different conditions (5 µg/mL of BSA, 10 µg/mL of human recombinant ApoE3, 1% heat-inactivated FBS, or 1% FBS + ApoE3) for 24 hours. (n=3/ per group) Culture media were collected to measure the concentration of free cholesterol using a colorimetric assay. Mean±SEM; *$P < 0.05$, ****$P < 0.0001$; one-way ANOVA.

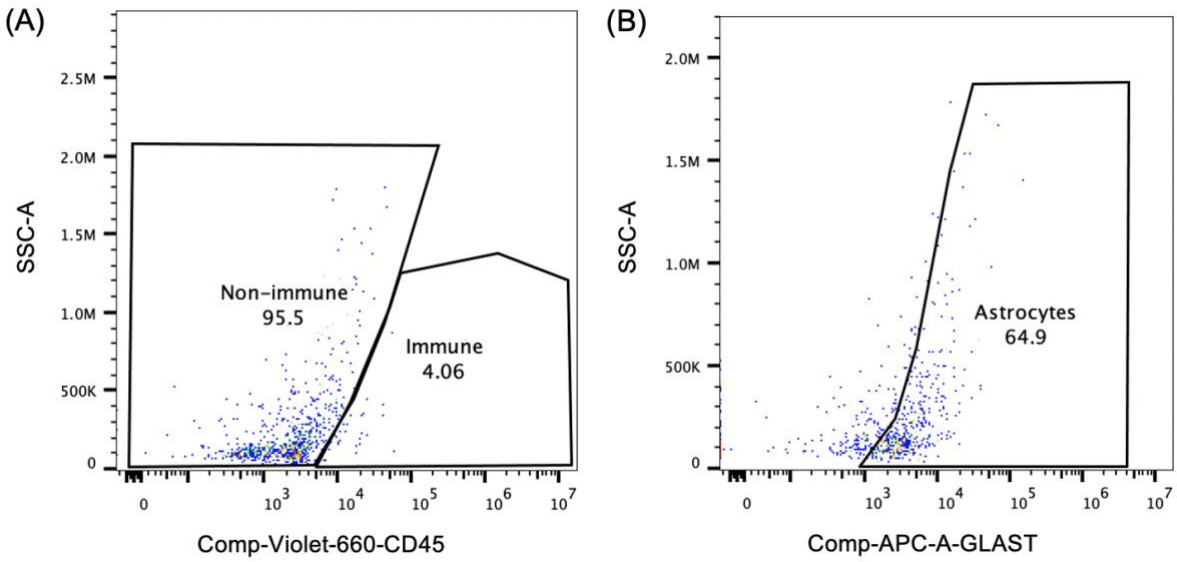

Figure 2.12: Dot plots of non-immune and astrocytic cells with their corresponding gating from flow cytometry analysis of cell cultures. To measure the purity of the primary astrocytes culture, cells were stained with **(A)** CD45-Violet-660 antibody to select for non-immune cells and **(B)** APC-GLAST antibody to select for astrocytes, gated within the non-immune cells.

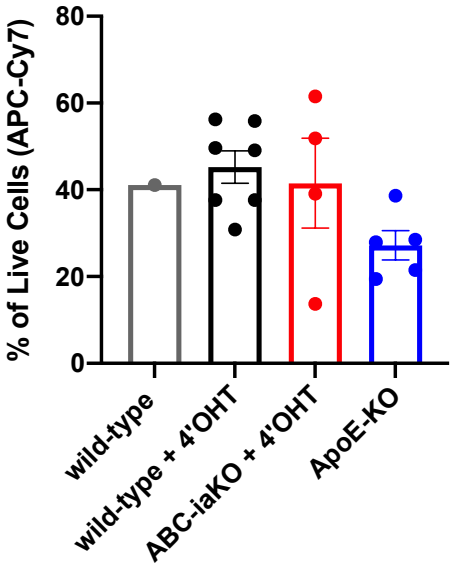

Figure 2.13: 4-hydroxytamoxifen does not affect cells' viability. Primary astrocytes from male ABC-iaKO and wild type mice (+ 4'OHT) were incubated with 1 µM of 4-hydroxytamoxifen for 24 hours. The percentage of live cells were measured using APC-Cy7-conjugated viability dye. Mean±SEM; one-way ANOVA.

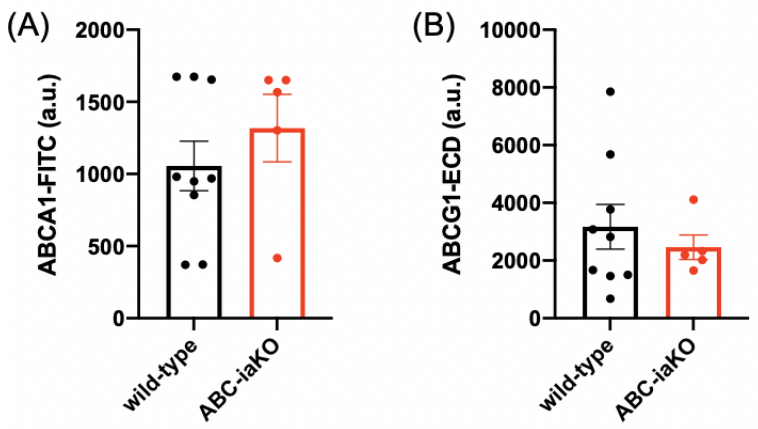

Figure 2.14: Testing *in-vitro* ABCA1 and ABCG1 cholesterol transporters knockdown. Primary astrocytes isolated from male wild-type (n=9) and ABC-iaKO (n=5) mice were treated with 1 µM of 4-hydroxytamoxifen for 24 hours to induce knockdown of ABCA1 and ABCG1 transporters. **(A)** ABCA1 transporters were measured using FITC-conjugated antibody and **(B)** ABCG1 transporters were measured using ECD-conjugated antibody for flow analysis. Integrated intensity values were calculated by multiplying frequency of positive cells with the geometric mean of fluorescence. Mean±SEM; unpaired t-test.

DISCUSSION

ABCA1 and ABCG1 cholesterol transporters in astrocytes play essential roles in regulating cholesterol distribution in the CNS. By conditionally deleting both ABCA1 and ABCG1 transporters in astrocytes, we found that ABC-iaKO mice experienced less allodynic pain upon nerve injury in comparison to wild-type mice. Different from microglia, removal of ABCA1 and ABCG1 cholesterol transporters in astrocytes was sufficient to protect the mice from spontaneous allodynia induced by cisplatin and paclitaxel. ABC-iaKO mice had significantly lower lipid rafts content in astrocytes and lipid droplets level in microglia compared to the wild-type mice. This finding aligns with the data that wild-type mice in the CIPN model treated with AIBP displayed reduced level of lipid rafts in microglia, proposing a possible explanation as to why ABC-iaKO mice were protected from cisplatin treatment but not wild-type mice. Further experiments would be needed to comprehensively study the association between lipid rafts in glial cells and neurons and other molecular mechanisms on pain induction.

Previous studies have shown that ABCA1 and ABCG1 transporters in astrocytes are responsible for cholesterol efflux to lipid-free lipoproteins and apolipoproteins, mainly ApoE, which carry cholesterol to neurons (Chen *et al.*, 2012; Karasinska *et al.*, 2013). Our data partly fit into the existing knowledge on the cholesterol regulation between astrocytes and neurons. ABC-iaKO mice displayed a trend toward lower lipid rafts content and level of lipid droplets in neurons. By removing ABCA1 and ABCG1 transporters in astrocytes, less cholesterol is being transported out of astrocytes, diminishing the amount of cholesterol being transported to neurons through lipoproteins and apolipoproteins. The lack of cholesterol availability for neurons may disrupt the functionality of neurons, desensitizing neurons from firing signals for pain perception, resulting in less allodynic pain. As shown in mice with constitutive deletion of ApoE,

compared to wild-type mice, they exhibited slightly higher mechanical thresholds and reduced levels of lipid droplets in neurons and microglia, demonstrating that ApoE is a key player that transports cholesterol to both neuronal and glial cells in the CNS.

One limitation of the study was the lack of a reliable assay to validate ABCA1 and ABCG1 knockdown. Although we could clearly observe the difference in mechanical paw-withdrawal thresholds between wild-type and ABC-iaKO mice, the failure in some experiments to demonstrate that both transporters were removed in astrocytes lowered the credibility of the flow analysis. Another limitation was that all the experiments were done only in male mice, excluding the factor of sex dimorphism between male and female. Past studies showed that male and female mice respond differently to the CIPN model, resulting in different degrees of mechanical allodynia (Woller *et al.*, 2019). Male mice experienced persistent allodynia after cisplatin administration throughout the experiment while female mice underwent initial allodynia and gradually returned to normal (Woller *et al.*, 2019). A follow up study would be helpful to distinguish the difference between male and female by examining the pain behavior and lipid composition of neurons in female mice with ABCA1 and ABCG1 deletion in astrocytes. In addition, studying the electrophysiology of the ABC-iaKO mice's neurons in response to mechanical stimuli could help the differences in neuronal nociceptive response.

METHODOLOGY

Induce knockdown of Cre-driver lines in-vivo

In the experiments, we induced knockdown of genes using the inducible *cre/lox* system. Following The Jackson Laboratory tamoxifen induction protocol, 10 mg/mL of tamoxifen (Sigma-Aldrich) was dissolved in corn oil overnight, shaken at 37ºC, wrapped in aluminum foil. When dissolved, tamoxifen was stored at 4ºC. *Cre*-inducible animals received 200 µL of tamoxifen injections intraperitoneally every 24 hours for five consecutive days.

Chemotherapy-induced neuropathic pain model

Animals received two intraperitoneal injections of either cisplatin (2.3 mg/kg/injection; Spectrum Chemical MFG, diluted in saline) or paclitaxel (8 mg/kg/injection; Tocris Bioscience; diluted in 1:1:8 solution of ethanol, cremophor EL, and saline) on Day 1 and 3 of the experiment. During the experiment, weight, behavioral changes, and mechanical allodynia were measured and recorded. Animals with excessive weight loss, 20% lowered than baseline measurement, or irregular behavior were euthanized. In this experiment, no animal needed euthanasia.

Intrathecal delivery of AIBP and saline

Animals were anesthetized using 5% isoflurane in oxygen during induction and 2% isoflurane in oxygen to maintain the phase of anesthesia. The lower back of the animals was shaven and disinfected before placing them in a prone posture. Using the thumb and forefinger to hold, the pelvis of the animals was held tightly to identify the L5 and L6 vertebrae. A 30G needle with 5 µL of solution (0. 5 µg/5 µL of AIBP) was inserted percutaneously on the midline for administration. A successful intrathecal injection delivery was noted by the observation of a tail

flick upon entry. The protocol of intrathecal injection was performed according to Hylden and Wilcox (1980).

Mechanical allodynia measurements

Before measurements, each animal was placed in a separate clear, bottomless, plastic cage on an elevated wire grid surface. Animals were acclimated for 10-15 minutes before the initiation of measurements. Following acclimation, von-Frey filaments (Bioseb) ranging from 2.44 to 4.31 (0.02-2.00 g) were pressed against the center of the hind paws using the up-down method to test whether the animals give an allodynic flinching response. The 50% probability of withdrawal thresholds of both hind paws were calculated and averaged for each entered time point of the experiment (Chaplan *et al.*, 1994).

Flow cytometry for ex-vivo assays

Spinal cords, brains, and dorsal root ganglion from the lumbar region were collected for flow cytometry. Tissues were processed using a Neural Tissue Dissociation kit (Miltenyi Biotec) to obtain single cell suspensions. To remove cell debris from cells, Debris Removal Solution kit (Miltenyi Biotec) was applied, following the manufacturer's protocol.

<u>Astrocytes isolation</u>

To isolate astrocytes in cells, anti-ACSA-2 MicroBeads (Miltenyi Biotec) were utilized to bind to astrocytic cells. Cells were passed through a LS column and a MACS Separator (Miltenyi Biotec) for separation. The flow through cells were used for measurement in microglia and

neurons. Cells bound onto Anti-ACSA-2 MicroBeads were flushed out of the LS column using PB buffer (PBS containing 1% BSA).

Lipid droplets, lipid rafts, and TLR4 dimerization measurements

Cells were incubated with 1 µg/mL FITC-conjugated BODIPY staining (Thermo Fisher Scientific) for 30 minutes on ice. After incubation, cells were washed and fixed with 4% formaldehyde for 10 minutes. Formaldehyde was removed and washed again before incubating with antibodies. Satellite and astrocytic cells were incubated in an antibody mix consisted of 1:1000 APC-Cy7-conjugated viability dye (Cell Signaling Technology) to select for live cells, 1:100 unconjugated GLAST antibody (NovusBio) to select for satellite or astrocytic cells, 1:250 ECD-conjugated CTB staining (Thermo Fisher Scientific) to select for lipid rafts content, 1:100 PE-conjugated MTS510 antibody (BioLegend) to select for TLR4/MD2 monomer, and 1:100 APC-conjugated SA15-21 antibody (BioLegend) to select for TLR4 receptors for 45 minutes on ice. After incubation, cells were washed and incubated with 1:250 secondary PECy7-conjugated anti-rabbit antibody for 30 minutes on ice. On the other hand, non-astrocytic cells were incubated in an antibody mix consisted of 1:1000 APC-Cy7-conjugated to measure cell viability, 1:100 Violet-660-conjugated CD45 antibody (BioLegend) to select for immune and non-immune cells, 1:100 PB450-conjugated CD24 and KO525-conjugated CD44 antibodies (BioLegend) to select for neuronal cells, 1:100 PerCp-Cy5.5-conjugated CD11b antibody (BioLegend) and PECy7-conjugated TMEM119 (Abcam) to select for macrophages and microglia, 1:250 ECD-conjugated CTB staining, 1:100 PE-conjugated MTS510 antibody, and 1:100 APC-conjugated SA15-21 antibody for 45 minutes on ice. After staining, all cells were washed and analyzed using a FACS flow cytometer.

Calculation of TLR4 dimers

Integrated intensity values of MTS510-PE (for TLR4/MD2 monomer) and SA15-21-APC (for total TLR4) were calculated by multiplying frequency of positive cells with the geometric mean of fluorescence. A ratio of TLR4/MD2 monomer and total TLR4 receptors were calculated. The calculated ratios of each sample were divided by the highest ratio and multiplied by 100 to resemble the maximum percentage of TLR4/MD2 monomers presented on the cells. The resulted number was then be subtracted from 100 to calculate the percentage of dimerized TLR4 receptors.

Cells

An immortalized astrocyte cell line from INK4a/ARF null mice was kindly donated by Dr. Frank Furnari's lab. Cells were cultured in astrocyte culture medium (1X DMEM (Cellgro), 10% heat-inactivated FBS (Omega), and 1% gentamycin sulfate solution (Omega)).

In-vitro lipidation assay

Five different conditions were created with phenol red-free Improved MEM medium (Corning) to add onto immortalized astrocytes for 24 hours of incubation at 37ºC: control, 10 µg/mL human recombinant ApoE3 (BioVision), 1% heat-inactivated FBS, 1% heat-inactivated FBS + 10 µg/mL human recombinant ApoE3, and 5 µg/mL of BSA. After incubation, culture media were removed and passed through 10kDa protein concentrator (Thermo Fisher Scientific) until the media reached around 10% of the original volume. All samples had similar final volumes. To ensure ApoE3 is adherent to the surface, a 96-well ELIZA plate coated with 5 µg/mL of ApoE antibody (BioVision) overnight were utilized. Coated wells were washed twice and blocked with

1% endotoxin-free BSA for one hour. After blocking, coated wells were washed twice again before incubating with new culture media each time for five times (one hour for the first and second, overnight for the third, and one hour for the fourth and fifth incubation) at room temperature. After five incubations with culture media, Total Cholesterol and Cholesterol Ester Colorimetric Assay Kit (BioVision) was used to detect the amount of free cholesterol in the culture media. Since this experiment was only interested in measuring the amount of free cholesterol, esterase enzyme was excluded in the protocol. To better detect the color difference between samples, reacted culture media were transferred to a 96-well clear flat bottom microplate (Corning) before measuring with a plate reader.

Primary astrocytes isolation

The whole brain tissue was collected from pups (P1-P15) and cut into small pieces using a sterilized small blade. To dissociate the tissue, the pieces are placed in 1X HBSS (Corning) containing 1 mM/mL of cysteine-HCl (Sigma-Aldrich) and 20 unit/mL of papain enzyme (Sigma-Aldrich) for one hour. After incubation, tissue was gently triturate and passed through a 70 µm cell strainer to remove large clumps of undissociated cells. Collected cells were plated in uncoated T25 flask with astrocyte culture medium and cultured in 5% CO_2 atmosphere at 37ºC. To select for astrocytes that are more adherent compared to other cells in the CNS, on Day 10-12 when astrocytes grew to confluence, the flask was put in a plastic Ziploc bag and placed on a shaker platform in horizontal position at 37ºC for 6-10 hours at the speed of 325 rpm. The media was changed once every seven days.

Induce knockdown of Cre-driver lines in-vitro

To induce knockdown in primary astrocytes isolated from animals with the *cre/lox* system, cells were incubated with 1 µM of 4-hydroxytamoxifen (Sigma-Aldrich) containing astrocyte culture medium for 24 hours at 37ºC. Unlike tamoxifen, 4-hydroxytamoxifen is less toxic and more suitable for cell culture.

Flow cytometry for in-vitro assays

To remove primary astrocytes off the flask, versene (Gibco^{TM}) was added to primary cells and incubated for a minute at 37ºC. Since astrocytes are more adherent to the surface, 0.5M of EDTA was added into the flask to help detach cells. Collected cells were separated into two parts for different flow cytometry measurements as described below.

Viability & purity tests

Half of the cells were incubated with 1 µg/mL FITC-conjugated BODIPY staining for 30 minutes on ice. After incubation, cells were washed and fixed with 4% formaldehyde for 10 minutes. Formaldehyde was removed and washed again before incubating with an antibody mix consisted of 1:1000 APC-Cy7-conjugated viability dye, 1:100 Violet-660-conjugated CD45 antibody to select for non-immune cells, 1:100 PB450-conjugated CD24 and KO525-conjugated CD44 antibodies to select for non-neuronal cells, and 1:100 APC-conjugated GLAST antibody (Miltenyi Biotec) to select for astrocytes on ice. After staining, cells were washed and analyzed using a FACS flow cytometer.

Knockout confirmation

Half of the cells were fixed with 4% formaldehyde for 10 minutes and washed before incubating with an antibody mix consisted of 1:100 APC-conjugated GLAST antibody and 1:100 FITC-conjugated ABCA1 antibody (Novus Biologicals) for 45 minutes on ice. Since ABCG1 cholesterol transporters tend to be internalized, cells were incubated with blocking buffer (1% BSA, 10% FBS, and 0.1% sodium azide) containing 1% of Triton™ X-100 to permeabilize the cells and 1:100 ECD-conjugated ABCG1 antibody (Novus Biologicals). After staining, cells were washed and analyzed using a FACS flow cytometer.

REFERENCES

Bruno, K.; Woller, S.A.; Miller, Y.I.; Yaksh T.L.; Wallace, M.; Beaton, G.; Chakravarthy, K. 2018. Targeting toll-like receptor-4 (TLR4)-an emerging therapeutic target for persistent pain states. *Pain.* 159:1908–1915. DOI:10.1097/j.pain.0000000000001306

Chaplan, S.R.; Bach, F.W.; Pogrel, J.W.; Chung, J.M.; Yaksh, T.L. 1994. Quantitative assessment of tactile allodynia in the rat paw. *Journal of Neuroscience Methods*. 53:55-63. DOI:10.1016/0165-0270(94)90144-9

Chen, J.; Zhang, X.; Kusumo, H.; Costa, L.G.; Guizzetti, M. 2012. Cholesterol efflux is differentially regulated in neurons and astrocytes: implications for brain cholesterol homeostasis. *Biochim. Biophys. Acta.* 1831:263-275. DOI:10.1016/j.bbalip.2012.09.007

Di Giorgio, F.B.; Carrasco, M.A.; Siao, M.C.; Maniatis, T.; Eggan, K. 2007. Non-cell autonomous effect of glia on motor neurons in an embryonic stem cell-based ALS model. *Nature Neuroscience.* DOI:10.1038/nn1885

Diaz Castro, B.; Gangwani, M.R.; Yu, X.; Coppola, G., Khakh, B.S. 2019. Astrocyte molecular signatures in Hunington's disease. *Science Translational Medicine.* 11:eaaw8546. DOI:10.1126/scitranslmed.aaw8546

Habib, N.; McCabe, C.; Medina, S.; Varshavsky, M.; Kitsberg, D.; Dvir-Szternfeld, R.; Green, G.; Dionne, D.; Nguyen, L.; Marshall, J.L.; Chen, F.; Zhang, F.; Kaplan, T.; Regev, A.; Schwartz, M. 2020. Disease-associated astrocytes in Alzheimer's disease and aging. *Nature Neuroscience.* 23:701-706. DOI:10.1038/s41593-020-0624-8

Hylden, J.L.K. and Wilcox, G.L. 1980. Intrathecal morphine in mice: A new technique. *European Journal of Pharmacology*. 67:2-3. DOI:10.106/0014-2999(80)90515-4

Ji, R.-R.; Nackley, A.; Huh, Y.; Terrando, N.; Maixner, W. 2018. Neuroinflammation and central sensitization in chronic and widespread pain. *Anesthesiology*. 129:343-366. DOI:10.1097/ALN.0000000000002130

Karasinska, J.M.; De Haan, W.; Franciosi, S.; Ruddle, P.; Fan, J.; Kruit, J.K.; Stukas, S.; Lütjohann, D.; Gutmann, D.H.; Wellington, C.L.; Hayden, M.R. 2013. ABCA1 influences neuroinflammation and neuronal death. *Neurobiology of Disease*. 54:445-455. DOI:10/1016/j.nbd.2013.01.018

Lee, Y.C.; Nassikas, N.J.; Clauq, D.J. 2011. The role of the central nervous system in the generation and maintenance of chronic pain in rheumatoid arthritis, osteoarthritis and fibromyalgia. *Arthritis Research & Therapy*. 13:211(2011). DOI:10.1186/ar3306

Li, X.; Zhang, J.; Li, D.; He, C.; He, K.; Xue, T.; Wan, L.; Zhang, C.; Liu, Q. 2021. Astrocytic ApoE reprograms neuronal cholesterol metabolism and histone-acetylation-mediated memory. *Neuron.* 109:957-970. DOI:10.1016/j.neuron.2021.01.005

Linetti, A.; Fratangeli, A.; Taverna, E.; Valnegri, P.; Francolini, M.; Cappello, V.; Matteoli, M.; Passafaro, M.; Rosa, P. 2010. Cholesterol reduction impairs exocytosis of synaptic vesicles. *Journal of Cell Science*. 123:595-605. DOI:10.1242/jcs.060681

Lolignier, S.; Eijkelkamp, N.; Wood, J.N. 2014. Mechanical allodynia. *Pflügers Archiv - European Journal of Physiology*. 467:133-139. DOI:10.1007/s00424-014-1532-0

Mahley, Robert W. 2016. Central Nervous System Lipoproteins: ApoE and regulation of cholesterol metabolism. *Atherosclerosis, Thrombosis, and Vascular Biology*. 7: 1305-1315. DOI:10.1161/ATVBAHA.116.307023

Miller, Y.I.; Navia-Pelaez, JMC.; Corr, M.; Yaksh, T.L. 2020. Lipid rafts in glial cells: role in neuroinflammation and pain processing. *Journal of Lipid Research.* 61:655–666. DOI:10.1194/jlr.TR119000468

Navia-Pelaez JMC; Choi, S.-H.; Capettini, L.S.A.; Xia, Y.; Gonen, A.; Agatisa-Boyle, C.; Delay, L.; Gonçalves dos Santos, G.; Catroli G.F.; Kim J.;, Lu, J.W.; Saylor, B.; Winkels, H.; Durant, C.P; Ghosheh, Y.; Beaton, G.; Ley, K.; Kufareva, I.; Corr, M.; Yaksh, T.L.; Miller, Y.I. 2021. Normalization of cholesterol metabolism in spinal microglia alleviates neuropathic pain. *Journal of Experimental Medicine* 2021. 218(7):e220202059. DOI:10.1084/jem.20202059

Nunes, V.S.; Cazita, P.M.; Catanozi, S.; Nakandakare, E.R.; Decreased content, rate of synthesis and export of cholesterol in the brain of ApoE knockout mice. *Journal of Bioenergetics Biomembranes.* 50:283-287. DOI:10.1007/s10863-018-9757-9

Seretny, M.; Currie, G.L.; Sena, E.S.; Ramnarine, S.; Grant, R.; MacLeod, M.R.; Colvin L.A.; Fallon, M. 2014. Incidence, prevalence, and predictors of chemotherapy-induced peripheral neuropathy: A systematic review and meta-analysis. *Pain*. 155:2461–2470. DOI:10.1016/j.pain .2014.09.020

Vergne-Seller, P. and Vertin, P. 2021. Chronic pain and neuroinflammation. *Joint Bone Spine*. 88(6):105222. DOI:10.106/j.jbspin.2021.105222

Wang, Q.; Liu, Y.; Zhou, J. 2015. Neuroinflammation in Parkinson's disease and its potential as therapeutic target. *Translational Neurodegeneration*. 4:19. DOI:10.1186/s40035-0150042-0

Wheeler, M.A. and Quintana, F.J. 2019. Regulation of astrocyte functions in multiple sclerosis. *Cold Spring Harbor Perspectives in Med.* 9:a029009. DOI:10.1101/cshperspect.a029009

Woller, S.A.; Choi, S.H.; An, E.J.; Low, H.; Schneider, D.A.; Ramachandran, R.; Kim, J.; Bae, Y.S.; Sviridov, D.; Corr, M. 2018. Inhibition of Neuroinflammation by AIBP: Spinal Effects upon Facilitated Pain States. *Cell Reports*. 23:2667-2677. DOI:10.1016/j.celrep.2018.04.110

Woller, S.A.; Corr, M.; Yaksh, T.L. 2019. Differences in cisplatin-induced mechanical allodynia in male and female mice. *European Journal of Pain*. 19(10):1476-1486. DOI:10.1002/ejp.679

Zajaczkowska R.; Kocot-Kepska, M.; Leppert, W.; Wrzosek, A.; Mika, J.; Wordliczek, J. 2019. Mechanisms of Chemotherapy-Induced Peripheral Neuropathy. *International Journal of Molecular Sciences*. 20(6):1451. DOI:10.3390/ijms20061451